Supplementary material for Nitroethane at high density: an experimental and computational vibrational study

Akio Yoshinaka[1,2], Serge Desgreniers[1], and Anguang Hu[2]

[1]Laboratoire de physique des solides denses, Department of Physics, University of Ottawa, Ottawa, Ontario, Canada K1N 6N5

[2]Defence R&D Canada Suffield Research Centre, Medicine Hat, Alberta, Canada T1A 8K6

Summary

The supplementary material section of this publication contains figures showing the comparison between DFT calculations and experimental results, additional pressure induced vibrational mode progressions and vibrational band shapes.

This section also incorporates the tabulated summary of all vibron modes of the free nitroethane (NE) molecule. A video animation file for the free NE molecule (in Gaussian output format[1]) has also been included.

Finally, video animations of the molecular motions within the monoclinic unit cell, as predicted by DFT calculations, for pressures ranging between 1.5 and 16 GPa are also included electronically in this section. The output format for these animations is compatible with the Molden[2] software.

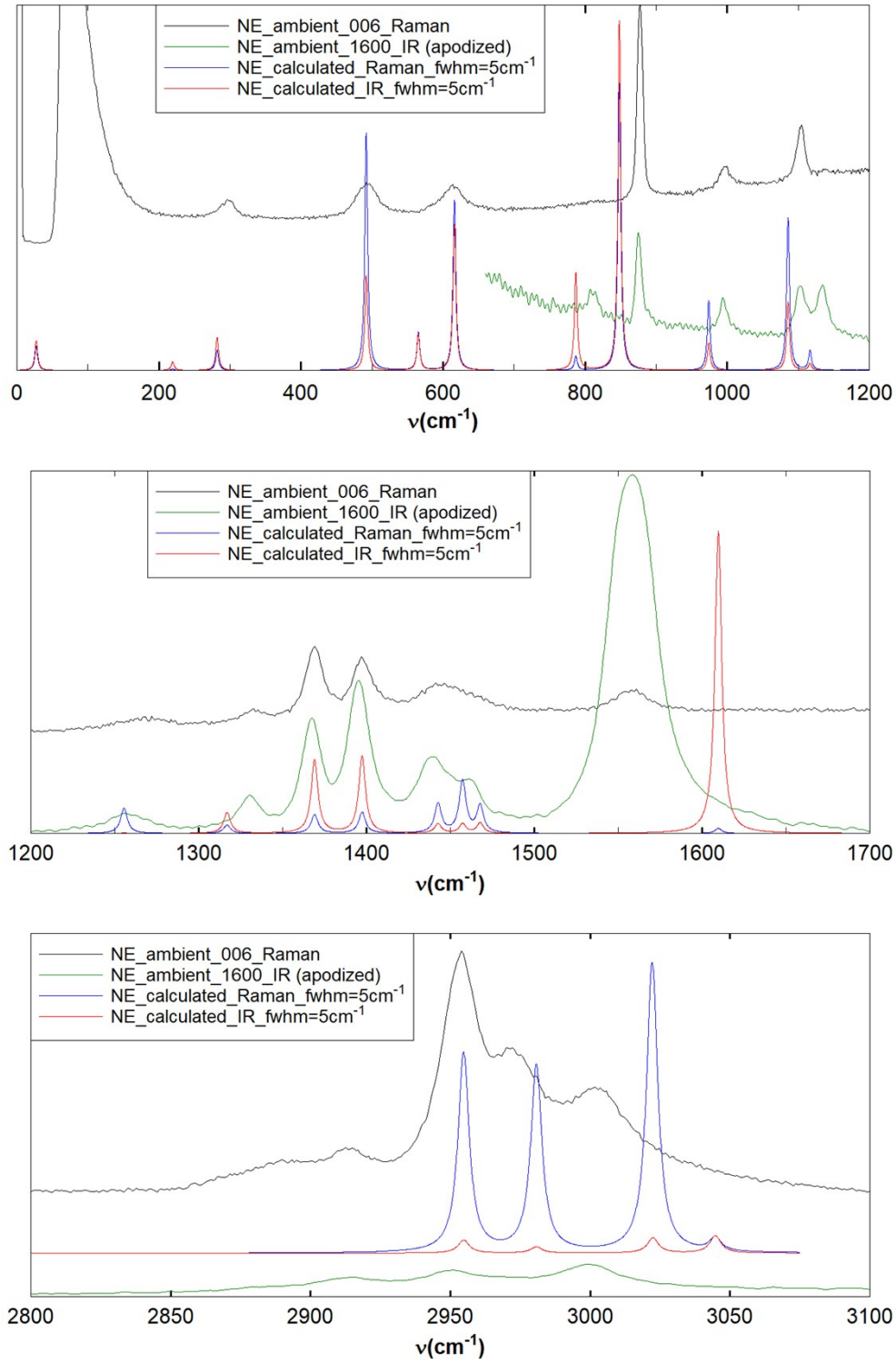

Figure S-1: Calculated vibrational spectra for NE free molecule compared with experimental Raman and IR vibrational spectra of ambient liquid NE. Calculated mode wavenumbers were scaled by 0.961.

Table S-1: Vibrational modes of nitroethane. Vibrational wavenumbers (in cm^{-1}) of liquid nitroethane under ambient temperature and pressure observed in this study compared to that from previous studies. Predicted mode wavenumbers and assignments are based on DFT calculations as described in the text. Each mode assignment typically results from vibrations in more than one bond; strongest contributions (stretching and/or angular deformation) appear first in bold based on relative magnitude of displacements. Wavenumbers without assignment are due to harmonics or combination bands.

Smith[3]			Geiseler[4]			Courtecuisse[5]		This work				
IR	IR	Raman	IR	Raman		Raman		IR	Raman	DFT calculation (B3LYP, 6-31G**)		
Vapor	Liq.	Liq.	Liq.	Liq.	Assignment	Liq.	Assignment	Liq.	Liq.	Single molecule	Assignment	Mode #
										27.1	**τ skeletal**	1
										219.3	**τ+ν_s CH_3**, τ skeletal	2
		295		298	-				297	281.9	**δ C-C-N**, **ρ NO_2**, ω CH_2, ρ(i.pl.) CH_3	3
	~495	491	493	494	**ρ NO_2**	494	**ρ NO_2**		492	491.8	**ρ+δ NO_2**, **δ C-C-N**, ρ(i.pl.) CH_3, ω CH_2, ν C-N, ν C-C, ν N-O	4
						614	**ω NO_2**		592	565.1	**ω+ν_s+δ NO_2**, **ρ+τ+ν_s CH_2**, τ skeletal	5
~621	616	614	614	615	**δ(sym)+ρ NO_2**	618	**δ(sym) NO_2**		614	616.0	**δ+ν_s NO_2**, **δ O-N-C**, **δ(i.pl.)+ν_s CH_3**, **δ C-C-N**, **ν C-N**, ρ(i.pl.) CH_3, ω+δ CH_2	6
807	810		810		**?**			811	811*	786.9	**ρ+τ+ν_s CH_2**, **ρ(o.pl.) CH_3**, **ω NO_2**, δ(o.pl.)+ν_s CH_3, τ skeletal	7
866												
876	875	874.7	878	878	**ν C-N**	878	**ν C-N**	875	877	848.2	**δ+ν_s NO_2**, **ν C-N**, **ρ(i.pl.) CH_3**, δ(i.pl.)+ν_s CH_3, ω+δ CH_2, ν C-C, δ O-N-C	8
884												
985												
996	993	993	992	996	**ν C-C**			995	997	973.9	**ρ(i.pl.) CH_3**, **ω+δ CH_2**, **ν C-C**, **ν C-N**, ν_s+δ NO_2, δ(i.pl.)+ν_s CH_3, δ C-C-N, δ O-N-C	9
1005												
1103	1103	1101.6	1101	1106	**ρ(o.pl.) CH_3**	1095–995	**ρ CH_3**	1103	1104	1085.6	**ρ(i.pl.) CH_3**, **ν C-C**, **δ C-C-N**, δ(i.pl.)+ν_s CH_3, ρ+ν_a NO_2, ω CH_2, ν C-N	10
1118												
~1124	1134		1131		**ρ(i.pl.) CH_3**			1134	1138	1116.6	**ρ+τ+ν_s CH_2**, **ρ(o.pl.) CH_3**, δ(o.pl.)+ν_s CH_3, ω NO_2, τ skeletal	11
~1150												
~1260	1255	1267	1253	1269	**τ CH_2**			1257	1265	1255.5	**τ+ν_s CH_2**, **ρ(o.pl.) CH_3**, δ(o.pl.)+ν_s CH_3, ω NO_2, τ skeletal	12
~1326	1330	1331	1330	1333	**ω CH_2**			1330	1332	1316.9	**ω+ν_s+δ CH_2**, **δ(i.pl.) CH_3**, **ρ(i.pl.) CH_3**, **ν C-N**, **ν C-C**, ν N-O, δ O-N-C, δ NO_2	13
~1352												

Table continues on next page.

Smith[3]			Geiseler[4]			Courtecuisse[5]		This work				
IR	IR	Raman	IR	Raman		Raman		IR	Raman	DFT calculation (B3LYP, 6-31G**)		
Vapor	Liq.	Liq.	Liq.	Liq.	Assignment	Liq.	Assignment	Liq.	Liq.	Single molecule	Assignment	Mode #
1366	1365	1366.5	1368	1370	**ν_s NO_2**	1395–1368	**ν_s NO_2**	1367	1369	1369.0	**δ(umbrella, i.pl.)+ν_s CH_3, ν_s+δ NO_2, ν C-N, δ+ω CH_2, δ O-N-C**, ν C-C	14
1379												
1397	1395	1395	1395	1399	**δ(sym) CH_3**			1395	1398	1397.4	**δ(umbrella, i.pl.)+ν_s CH_3, ν C-C, ν C-N, ω+δ CH_2, ν_s+δ NO_2, δ O-N-C**	15
1406												
~1440	1441	1440	1440	1440	**δ(sym) CH_2**	1440	**δ(sym) CH_3**	1439	1444	1442.6	**δ+ν_s CH_2, ν C-C**, δ(i.pl.) CH_3, ν_s+δ NO_2, δ C-C-N, δ O-N-C	16
1458	~1452	1456	1450		**?**			1452	1453	1457.3	**δ(o.pl.)+ν_s CH_3**, τ skeletal	17
~1480	~1465		1463	1463	**δ CH_3+CH_2**			1463	1465	1467.7	**δ(i.pl.)+ν_s CH_3, δ+ω CH_2**, ν C-N, ν C-C	18
1573	1560	1554	1559	1559	**ν_a NO_2**	1555	**ν_a NO_2**	1558	1558	1609.7	**ν_a+δ NO_2, δ O-N-C, δ C-C-N, ω+δ CH_2**, δ(umbrella, i.pl.) CH_3, ν C-N, ν C-C	19
1588												
	1862											
	1946											
	1976											
	2075											
	2128											
	2208											
	2247											
	2315											
	2358											
~2435	2420											
	~2470											
	2560											
	2650								2652			
~2750	2750	2749							2750			
		2890	2880	2889	-			2882	2889			
		2912						2913	2913			
2950	2950	2951	2903	2944	**ν_s CH_3+CH_2**	2950	**ν_s CH_3**	2950	2953	2954.7	**ν_s+δ(i.pl.) CH_3**, ν C-C, δ C-C-N, ω+ν_s CH_2	20
								2970	2973	2980.7	**ν_s+δ CH_2**, ν_a(i.pl.) CH_3, δ C-C-N, ν C-C	21
		2971	2938	2971	**ν_a CH_2**				3001	3022.0	**ν_a CH_2, ν_a(o.pl.) CH_3**, τ skeletal	22
3010	3000	3001	2990	3013	**ν_a+ν_s CH_3**			3000	3004	3022.4	**ν_a(i.pl.) CH_3, ν_s CH_2**, δ C-C-N, δ O-N-C	23
									3030	3044.7	**ν_a(o.pl.) CH_3, ν_a CH_2**, τ skeletal	24
	~3225											
	3600											
	3680											
	4100											
	4270											
	4430											

τ, torsion; δ, bending/scissoring; ρ, rocking; ω, wagging; ν, stretching (ν_s, symmetric stretching; ν_a, asymmetric stretching)
i.pl., deformation is symmetric with, or in the C-C-N-O_2 plane of symmetry
o.pl., deformation is asymmetric with, or out of the C-C-N-O_2 plane of symmetry
* Weak, peak requires fitting before baseline removal

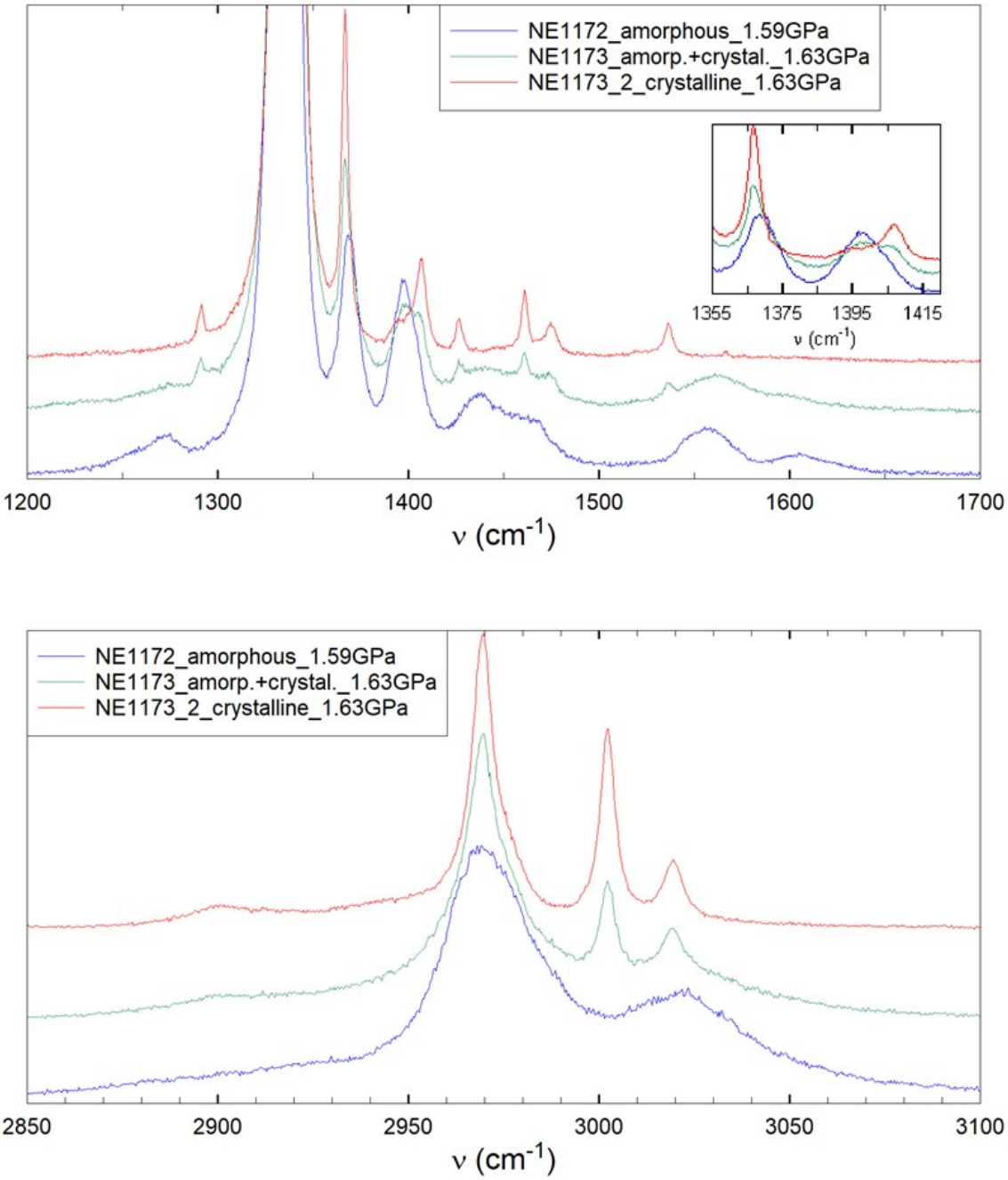

Figure S-2: Raman vibrational spectra of NE at ~1.6 GPa in the high fingerprint (top for $\nu \lesssim 1500\text{cm}^{-1}$) and functional group (top for $\nu \gtrsim 1500\text{cm}^{-1}$ and bottom) regions.

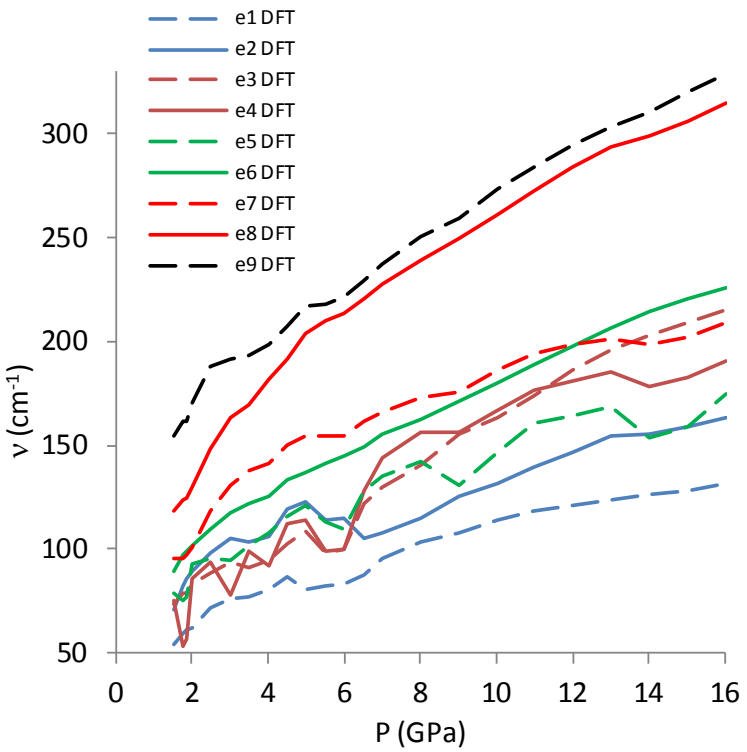

Figure S-3: Calculated pressure-induced vibrational mode shifts for external modes of nitroethane in the NE crystalline phase.

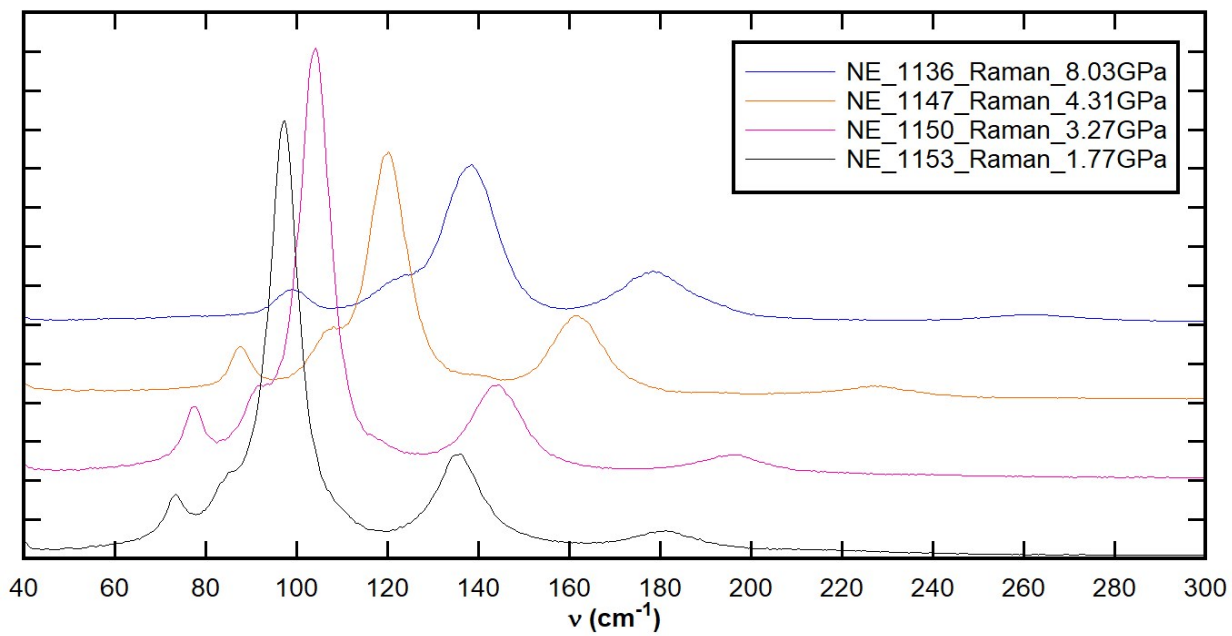

Figure S-4: Observed Raman vibrational band shape in the low wavenumber range at various pressures.

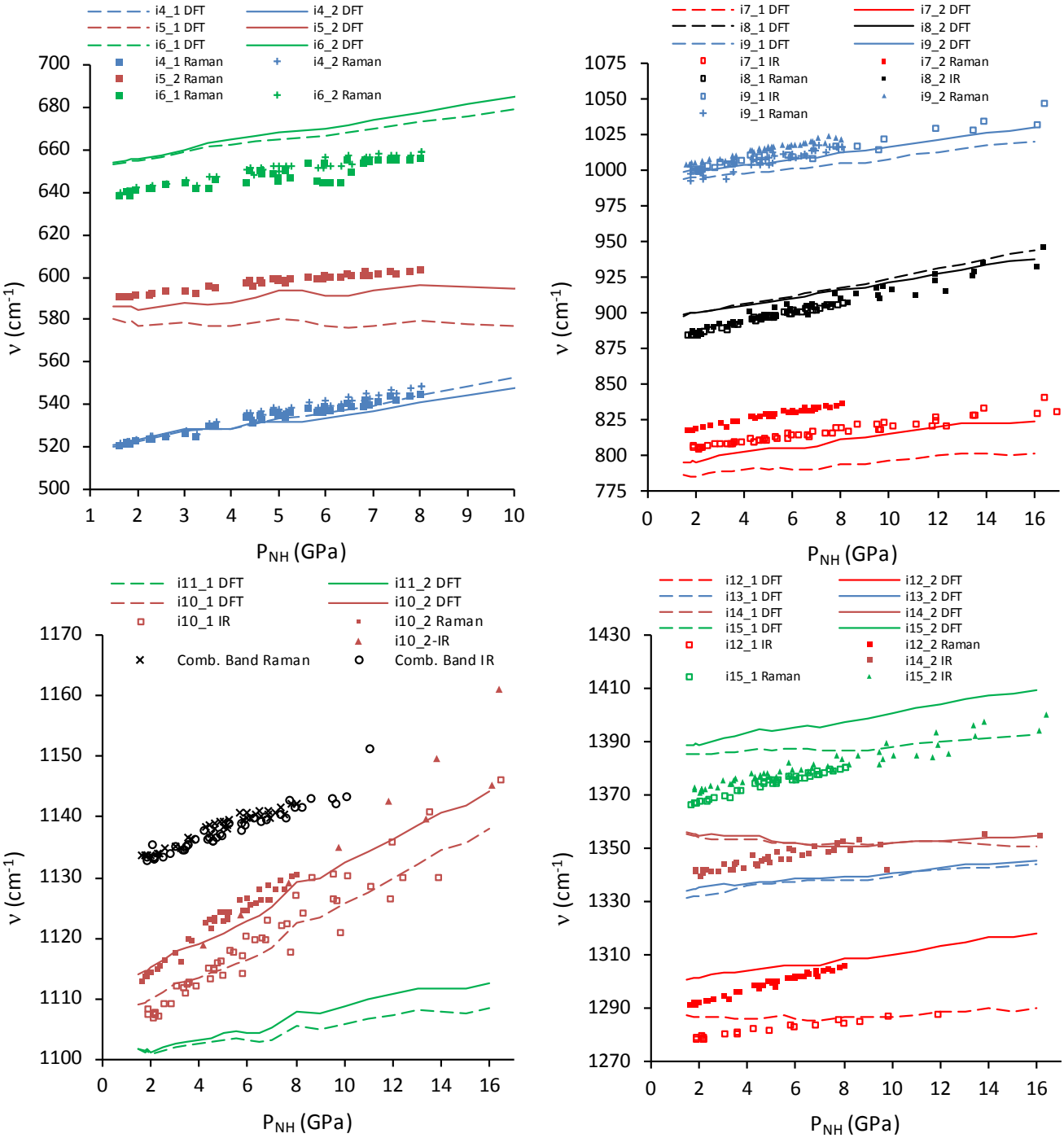

Figure S-5: Vibrational mode progressions as a function of pressure for assigned modes in the fingerprint region. Calculated (DFT) mode progressions for both Davydov components have been scaled as described in the text. Prefixes "e" and "i" denote external and internal modes, respectively. Suffixes "_1" and "_2" denote each Davydov components.

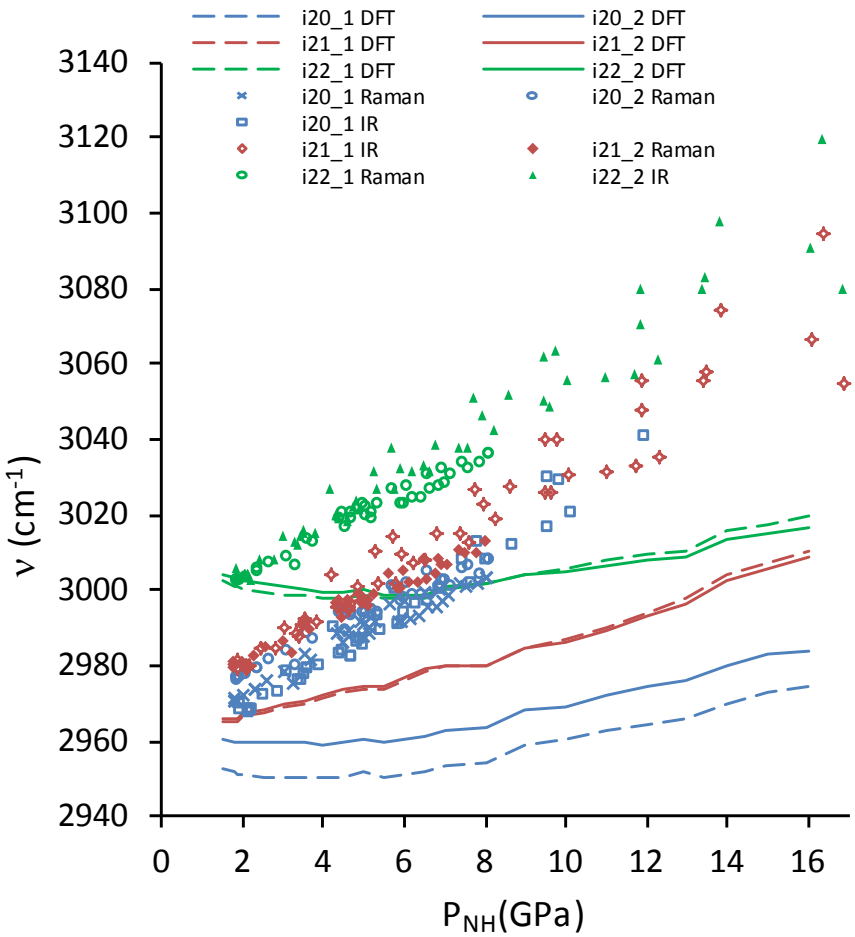

Figure S-6: Vibrational mode progression as a function of pressure for modes i23 and i24 in the functional group region. Calculated (DFT) mode progressions for both Davydov components have been scaled as described in the text. Prefixes "e" and "i" denote external and internal modes, respectively. Suffixes "_1" and "_2" denote each Davydov components.

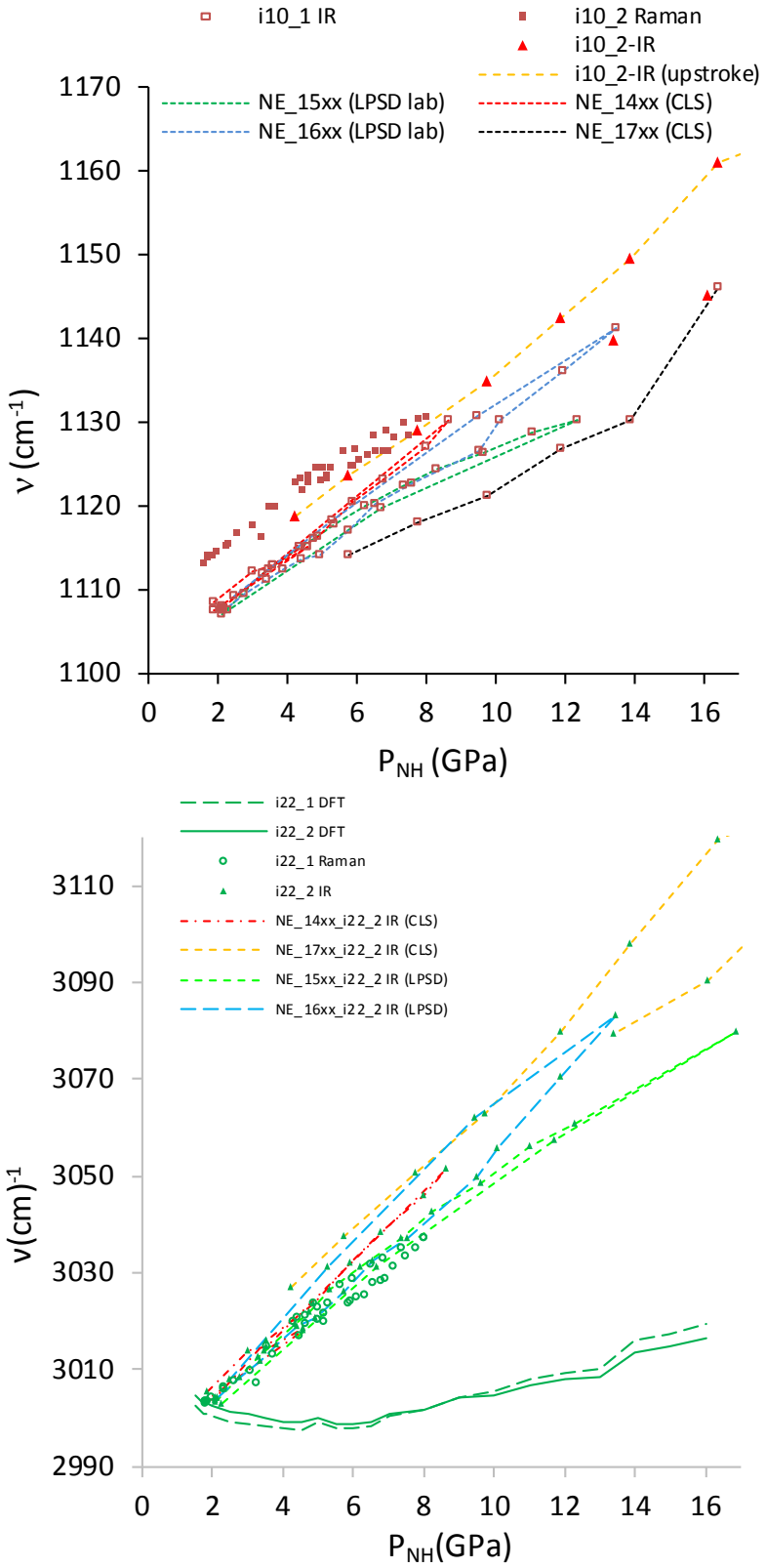

Figure S-7: Pressure induced evolutions of modes i10 (top) and i22 (bottom). Dotted lines highlight four different IR sample loading. Subscript "NH" denotes the use of a non-hydrostatic ruby pressure standard, as described in the text.

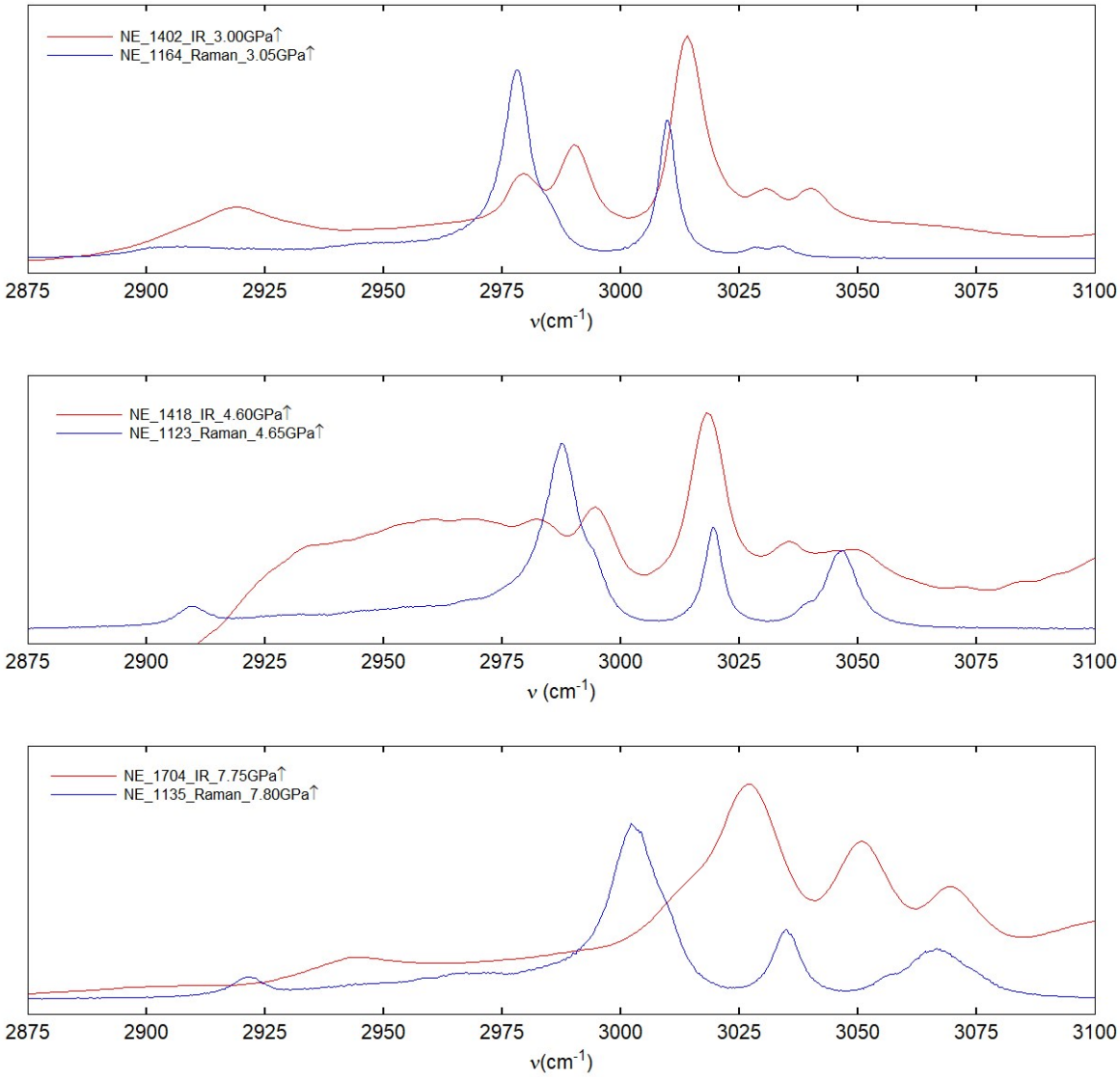

Figure S-8: Comparison between Raman and IR vibrational spectra in the functional group region between pressures ~3.0-7.8 GPa. Legend symbol "↑" denotes a spectrum obtained during the pressure upstroke.

Supplementary References

[1] R. Dennington, T. Keith, and J. Millam, in *GaussView Version 5.0.8* (Gaussian, Inc. Wallingford CT 06492 USA), 2009).
[2] G. Schaftenaar, and J. H. Noordik, Journal of Computer-Aided Molecular Design **14** (2000) 123.
[3] D. C. Smith, C. Y. Pan, and J. R. Nielsen, The Journal of Chemical Physics **18** (1950) 706.
[4] G. Geiseler, and H. Kessler, Berichte der Bunsengesellschaft für physikalische Chemie **68** (1964) 571.
[5] S. Courtecuisse *et al.*, The Journal of Chemical Physics **108** (1998) 7350.